REVISED LIFETIME OF THE $11/2^-$ STATE IN ^{45}Sc VIA COULOMB EXCITATION*

M. Matejska-Minda[a], P.J. Napiorkowski[b], R. Kumar[c]
M. Saxena[b,d], S. Dutt[e], A. Agarwal[f], I. Ahmed[c]
S. Bhattacharya[g], A. Jhingan[c], J. Kaur[h], M. Kicińska-Habior[i]
M. Kumar[c], S. Kumar[c], D. Kumar[j], V. Nanal[k], R. Palit[k]
N.K. Rai[l], M. Shuaib[e], A. Sood[m], A. Stolarz[b], T. Trivedi[g]
A.K. Tyagi[l], R.K. Bhowmik[c], H.J. Wollersheim[n]

[a]Institute of Nuclear Physics Polish Academy of Sciences, Kraków, Poland
[b]Heavy Ion Laboratory, University of Warsaw, Warszawa, Poland
[c]Inter University Accelerator Centre, New Delhi, India
[d]Department of Physics and Astrophysics, University of Delhi, New Delhi, India
[e]Department of Physics, Aligarh Muslim University, Aligarh, India
[f]Department of Physics, Bareilly College, Bareilly, India
[g]Department of Pure and Applied Physics, Guru Ghasidas University
Bilaspur, India,
[h]National Institute for Physics and Nuclear Engineering (IFIN-HH)
Bucharest-Măgurele, Romania
[i]Faculty of Physics, University of Warsaw, Warszawa, Poland
[j]Department of Physics, Indian Institute of Technology Roorkee, Roorkee, India
[k]Department of Nuclear and Atomic Physics, TIFR, Mumbai, India
[l]Department of Physics, Banaras Hindu University, Varanasi, India
[m]Department of Physics, Indian Institute of Technology Ropar, Rupnagar, India
[n]GSI, Darmstadt, Germany

A Coulomb-excitation measurement to study low-energy electromagnetic properties of ^{45}Sc has been performed at the IUAC facility in New Delhi, India using a 70 MeV ^{32}S projectile from the 15UD tandem accelerator. The preliminary value of the reduced transition probability $B(\mathrm{E2}; 11/2^- \rightarrow 7/2^-)$ and the resulting lifetime for the $11/2^-$ state at 1237 keV were determined using the GOSIA code.

---

1. Introduction

A full understanding of the nuclear structure and atomic nucleus features is hindered by the complexity of the nuclear force, which is composed of many different terms. Nuclei with an excess or deficiency of neutrons with respect to the doubly-magic isotopes are an effective laboratory to understand the role of the various components of the nuclear Hamiltonian. The ^{45}Sc nucleus, situated in the nuclear chart above the doubly-magic ^{40}Ca, has 1 additional proton and 4 neutrons beyond the $N = Z = 20$ shell closure. Odd-mass nuclei in the lower part of the $f_{7/2}$ shell provide striking examples of non-closure effects of the $N = Z = 20$ shells, which result in the occurrence of many low-lying positive parity "intruder" states, *e.g.* in ^{43}Sc, ^{45}Sc, ^{47}Sc, ^{45}Ti, and ^{49}V [1, 2]. Although in this region the ground states are predominantly spherical, at higher values of spin, well-deformed rotational bands are present. In ^{45}Sc, the negative-parity states built on the $7/2^-$ ground state exhibit a spherical structure, while a well-deformed rotational-like band is formed upon the $3/2^+$, $T_{1/2} = 318$ ms isomeric state [3].

The structure of odd-mass Sc isotopes is particularly interesting because of the coexistence of positive-parity and negative-parity bands near the ground state. This is inconsistent with the naive shell-model picture, which suggests only negative-parity states near the ground state for the scandium isotopes. This happens when one considers only the fp configuration space for the valence particles, without ^{40}Ca core excitations. For example, ^{45}Sc has a degenerated $3/2^+$ positive-parity state only 12.4 keV above the $7/2^-$ ground state. A Coulomb-excitation measurement can provide new valuable information on the electromagnetic properties of low-lying states in ^{45}Sc, which will contribute towards a better understanding of the role played by single-particle degrees of freedom in creating nuclear collectivity. The Coulomb-excitation experiments of scandium isotopes have been performed with beams of protons [4], and also with ^{16}O and ^{35}Cl ions [5, 6] in the early 1970s. However, the measuring techniques and data analysis methods did not allow for the determination of essential data such as signs and magnitudes of quadrupole moments for the $3/2_1^+$, $5/2_1^+$ and $7/2_1^+$ states, and the transitional electromagnetic matrix elements between low-lying states inside the ground state and isomeric band. The Coulomb-excitation measurement of ^{45}Sc was performed to determine the $B(\text{E3}; 7/2^- \rightarrow 3/2^+)$ and $B(\text{E3}; 7/2^- \rightarrow 5/2^+)$ transition probabilities (upper limit reported in Ref. [7]), as well as other transitional electromagnetic matrix elements for low-lying states.

In the present paper, we report the preliminary results regarding the $B(\text{E2}; 11/2^- \rightarrow 7/2^-)$ and the resulting lifetime for the $11/2^-$ state at 1237 keV that were determined using the GOSIA code [8].

2. Experimental details

The Coulomb-excitation experiment to study ^{45}Sc was performed in November 2017 at the Inter University Accelerator Centre, New Delhi, India. A ^{32}S beam of 70 MeV energy, delivered from the 15UD tandem accelerator, was scattered on a 1 mg/cm^2 ^{45}Sc target. The γ rays depopulating Coulomb-excited states in ^{45}Sc were detected by four clover detectors in coincidence with forward scattered ions. Clover detectors were placed at the distance of 18 cm from the target at the $\theta_{LAB} \sim 145°$ laboratory angle with respect to the beam direction. The scattered beam particles and the recoiling target nuclei were detected in the position-sensitive Annular Parallel Plate Avalanche Counter (APPAC) [9]. The APPAC is mounted in the forward direction having angular coverage from 15° to 45° in a cone around the beam axis. The front layer of the gas-filled APPAC particle detector is divided into 16 radial segments to provide ϕ angle, whereas the backward placed delay lines provide θ scattering angle of the reaction products.

For the given configuration and projectile detection, the opening angle of the APPAC particle detector corresponds to an angular coverage of $\theta_{CM} = 25°–75°$ for beam ions and $\theta_{CM} = 105°–155°$ for target nuclei, in the center-of-mass system.

The data were registered under a coincidence condition that at least one γ ray was detected in the clover array with exactly one scattered ion detected in the APPAC particle detector.

3. Data analysis and results

Collected data were analyzed using the ROOT-based Go4 software package [10]. Individual timing gates were applied for each crystal of clover detectors and ϕ segments of APPAC to reduce the background radiation. The total Doppler-corrected and background-subtracted γ-ray spectrum of ^{45}Sc, summed over all crystals and all segments of the APPAC particle detector, is shown in Fig. 1. For a given θ_{LAB} angle, both target recoils and scattered beam projectiles were registered, corresponding to different center-of-mass scattering angles. Thus, one peak component of the double-peak structure seen in Fig. 1 arises from the distant collision events (projectile detected in APPAC), while the second one from the close collision events (target nuclei detected in APPAC). At the same time, Cline's "safe energy" criterion ensuring the purely electromagnetic interaction between the colliding nuclei [11] was fulfilled only for the distant collision events, up to scattering angle $\theta_{LAB} = 65°$ in the laboratory frame.

When applying Doppler correction for the projectile detection, the wrongly corrected close collision events affect the intensity of the γ-ray transitions resulting from the distant collision events. Therefore, to take

into account only events resulting from the "safe" Coulomb excitation for the analysis, we selected only those combinations of crystals and APPAC segments in which this double-peak structure is well-separated, which are:

— Clover 1 ($\theta_\gamma \sim 145°$, $\phi_\gamma \sim 45°$) and $\phi_p = 135°$–$270°$,
— Clover 2 ($\theta_\gamma \sim 145°$, $\phi_\gamma \sim 145°$) and $\phi_p = 90°$–$202.5°$,
— Clover 3 ($\theta_\gamma \sim 145°$, $\phi_\gamma \sim -45°$) and $\phi_p = 0°$–$22.5°$ and $225°$–$360°$,
— Clover 4 ($\theta_\gamma \sim 145°$, $\phi_\gamma \sim -145°$) and $\phi_p = 0°$–$112.5°$ and $315°$–$360°$.

In this way, we could eliminate the contamination from the "unsafe" Coulomb excitation from the experimental yields.
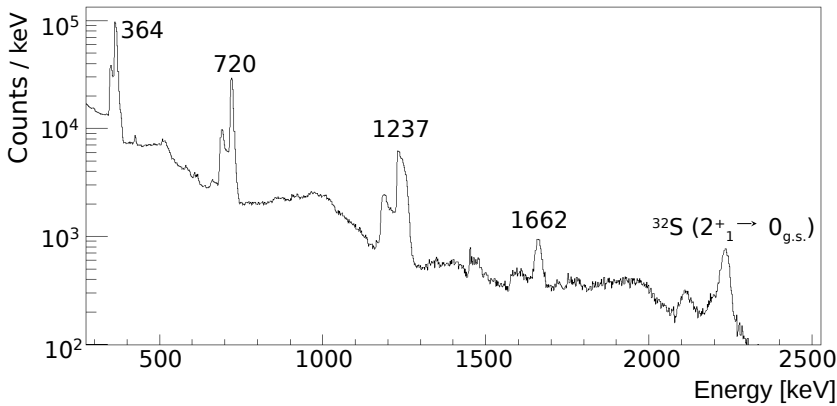

Fig. 1. Total Doppler-corrected and background-subtracted γ-ray energy spectrum of ^{45}Sc, observed in the present Coulomb-excitation experiment. Doppler correction was applied for the projectile ions registered in APPAC particle detector. Peaks are marked with their energy in keV.

As an example, Fig. 2 shows the γ-ray energy spectrum for clover 3 in coincidence with 7 segments of APPAC (covering angular range from $\phi_p = 0°$–$22.5°$ and $225°$–$360°$). Resulting low-energy part of the ^{45}Sc level scheme depicting γ-ray transitions observed in the present Coulomb-excitation experiment is shown in Fig 3.

The Coulomb-excitation analysis was performed using the least-squares fitting code GOSIA. Experimental data were divided into four separate data sets, one for each clover and the selected range of APPAC segments (listed above), in which the double-peak structure is well-separated.

For ^{45}Sc, the known lifetimes of the $3/2_1^-$, $5/2_1^-$, $9/2_1^-$, $3/2_1^+$ and $5/2_1^+$ states and the branching ratios for the $3/2_1^-$ and $9/2_1^-$ decays [12], as well as δ(E2/M1) mixing ratios for the 425 keV, 720 keV and 1662 keV transitions, were used as additional data points in the GOSIA fit.
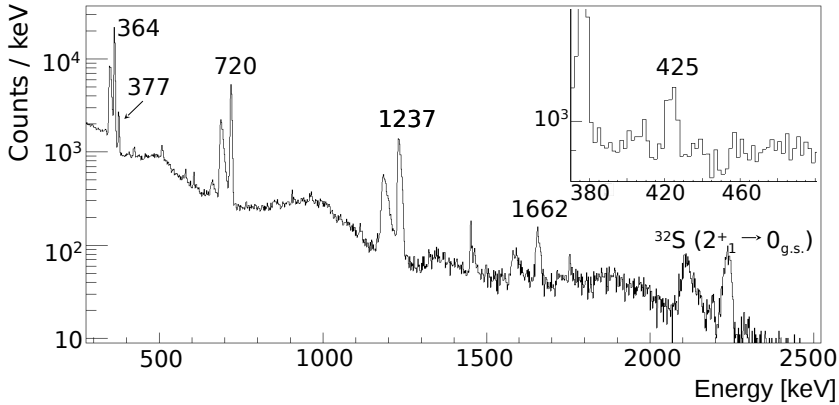
Fig. 2. γ-ray energy spectrum following the Coulomb excitation of ^{45}Sc, registered in clover 3 in coincidence with scattered ions detected in the selected range of APPAC segments (listed in the text). Doppler correction was applied for the projectile ions registered in the APPAC particle detector. The inset contains the low-energy part of the same spectrum zoomed on the 425 keV transition. Peaks are marked with their energy in keV.
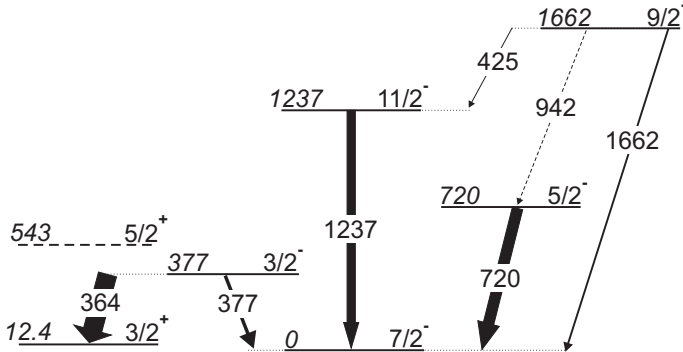

Fig. 3. Low-energy part of the level scheme of ^{45}Sc, widths of the arrows correspond to the γ-ray intensities observed in the present Coulomb-excitation experiment. The 942 keV transition and 543 keV level (dashed line) were not observed in the present experiment, but they were included in the Coulomb-excitation data analysis.

While constructing the additional spectroscopic data set for ^{45}Sc, it was noticed that the literature lifetime values for the $11/2^-$ state at 1237 keV vary from $0.12\,(8)$ ps [13] up to $2.4\,(+10, -6)$ [14] (see Table I). Therefore, due to such a large discrepancy, the lifetime value for that state was not included in the analysis as an additional spectroscopic data point to be fitted. In the GOSIA code, a standard χ^2 function was constructed from

the γ-ray yields observed in the Coulomb-excitation experiment and those calculated from a set of matrix elements between all relevant states. As a result of the minimization process, a set of matrix elements was found that reproduces all experimental γ-ray yields, as well as the other additional data included in the analysis.

TABLE I

Literature half-lives of the $11/2^-$ state at 1237 keV in ^{45}Sc.

$T_{1/2}$ [ps]	Reaction	References
0.12 (8)	$(n, n'\gamma)$	[13]
2.4 (+10, −6)	$(\alpha, p\gamma)$	[14]
1.60 (0.34)	$(p, p'\gamma)$	Average of [15–18]
1.80 (0.10)	(γ, γ')	NNDC adopted value [19]

Preliminary results determined in the course of present Coulomb-excitation analysis are $B(\text{E2}; 11/2^- \to 7/2^-) = 74 \pm 5 \; e^2\text{fm}^4$ and the resulting lifetime for the $11/2^-$ state at 1237 keV, $\tau = 3.83 \pm 0.27$ ps ($T_{1/2} = 2.65 \pm 0.18$ ps). The diagonal matrix element of the $11/2^-$ state at 1237 keV as well as the feeding of this state via one and second-step excitation (through the $9/2^-$ state at 1662 keV) was included in the analysis. The obtained value is closest to the outcome of the $(\alpha, p\gamma)$ reaction measurement [14].

Further analysis aims to determine the electromagnetic properties for all Coulomb-excited states in the ^{45}Sc isotope. Subdivision of the experimental data based on the projectile scattering angle will help to unravel contributions from various excitation paths. Moreover, a combined analysis of the present data with our previously performed ^{45}Sc Coulomb-excitation measurement at the Heavy Ion Laboratory, University of Warsaw [7] aims to disentangle contributions from the $B(\text{E3}; 7/2^- \to 3/2^+)$ and $B(\text{E3}; 7/2^- \to 5/2^+)$ transition probabilities.

REFERENCES

[1] J. Styczeń et al., Nucl. Phys. A 262, 317 (1976).

[2] P. Bednarczyk et al., Eur. Phys. J. A 2, 157 (1998).

[3] M. Avgoulea et al., J. Phys. G: Nucl. Part. Phys. 38, 025104 (2011).

[4] D.C. Tayal, K.P. Singh, H.S. Hans, *Phys. Rev. C* **34**, 1262 (1986).

[5] A.E. Blaugrund *et al.*, *Phys. Rev.* **159**, 926 (1967).

[6] M.D. Goldberg, B.W. Hooton, *Nucl. Phys. A* **132**, 369 (1969).

[7] M. Matejska-Minda *et al.*, *Acta Phys. Pol. B* **49**, 567 (2018).

[8] T. Czosnyka, D. Cline, C.Y. Wu, *Bull. Amer. Phys. Soc.* **28**, 745 (1983),
     http://slcj.uw.edu.pl/en/gosia-code/

[9] A. Jhingan *et al.*, *Nucl. Instrum. Methods Phys. Res A* **922**, 209 (2019).

[10] https://www.gsi.de/go4.htm

[11] D. Cline, *Annu. Rev. Nucl. Part. Sci.* **36**, 683 (1986).

[12] National Nuclear Data Center, Brookhaven, https://www.nndc.bnl.gov/

[13] M.K. Georgieva *et al.*, *Fiz. Elem. Chastits At. Yadra* **20**, 930 (1989).

[14] J. Chevallier, B. Haas, N. Schulz, M. Toulemonde, *J. Phys.* **37**, 303 (1976).

[15] N.J.A. Rust *et al.*, *Nucl. Phys. A* **219**, 232 (1974).

[16] J.J. Buitendag *et al.*, *Z. Phys. A* **295**, 107 (1980).

[17] M. Rahman, H.P. Nottrodt, F. Rauch, *Nucl. Phys. A* **401**, 253 (1983).

[18] D.K. Avasthi *et al.*, *Acta Phys. Pol. B* **16**, 847 (1985).

[19] F.R. Metzger, *Phys. Rev. C* **12**, 312 (1975).